Ordered Micelle Structuring in Thin Films Formed from Anionic Surfactant Solutions

I. Experimental

A. D. NIKOLOV[1] AND D. T. WASAN[2]

Department of Chemical Engineering, Illinois Institute of Technology, Chicago, Illinois 60616

Received March 7, 1988; accepted January 3, 1989

Reflected light micro-interferometry was used to observe stratification (i.e., the kinetics of layered structuring) in thinning foam films formed from micellar solutions of sodium *n*-alkyl sulfates at concentrations much lower than those at which liquid crystalline structures form in bulk solutions. The effects of surfactant concentration and chain length, added electrolyte, and capillary pressure on the step-wise jump transition thicknesses have been investigated. We have further conducted a model study with films formed from aqueous dispersions of latex particles. In similar fashion to those formed from micellar solutions, the thinning films changed thickness with regular step-wise jump transitions, and the films exhibited a number of metastable equilibria. These observations verify that the stratification of thin liquid films can be explained as a layer-by-layer thinning of ordered structures of micelles or colloidal particles formed inside the film. The stratification–nonstratification phase diagram is presented for anionic micelles and is similar to the order–disorder phase diagram for latexes. In the accompanying paper (Part II) we show that the phenomenon of stratification and ordered micellar structures is governed by the long range electrostatic repulsion beteen the ionic micelles and the restricted volume of the film. This present study provides evidence, for the first time, for the presence of structural forces in thin films with thicknesses on the order of 100 nm and strongly suggests that the free liquid film dynamics may be used as a probe to study the ordering in, and stability of, microheterogeneous systems.

INTRODUCTION

Johnnott (1) and Perrin (2) long ago observed the phenomenon of step-wise thinning of liquid foam films. This phenomenon, called stratification, was later observed and investigated by many authors, with both foam films (3–6) and emulsion films (7–9). Hachisu, Kobayashi, and Kose (10) established experimentally that latex particles in an aqueous solution form ordered structures (solid-like arrangements of latex particles). This finding awoke considerable interest: relative to the size of the particles, the interparticle distances in the latex-ordered structures are too large for the van der Waals forces to be important. The classical DLVO theory (11, 12) thus cannot explain the ordering in such systems as a balance of van der Waals forces and electrostatic forces at the secondary minimum of the interaction energy. The ordering in these structures must then be entirely due to the electrostatic interactions. Many researchers have performed studies both theoretical (13–22) and experimental (23–27) to explain this phenomenon.

Our aim here is to present some recent experimental results for stratifying films formed from anionic surfactants such as sodium *n*-alkyl sulfates and to offer a physical explanation. These results show that the micellar structures inside a stratifying film resemble the latex-ordered structures observed by Hachisu *et al.* (10) in bulk solutions. Moreover, as re-

[1] Present address: Laboratory of Thermodynamics and Physicochemical Hydrodynamics, Faculty of Chemistry, University of Sofia, 1126 Sofia, Bulgaria.

[2] Author to whom correspondence should be addressed.

0021-9797/89 $3.00

ported below, films formed from latex solutions also exhibit stratification. For this reason, one can conclude that both phenomena (stratification of thin liquid films and ordering in latex solution) likely have the same physical origin.

EXPERIMENTAL STUDY OF STRATIFYING FILMS

(a) Characterization of Micellar Solutions

For surfactants such as sodium *n*-alkyl sulfates (with more than eight carbon atoms in the chain), micelles are formed beyond the critical micelle concentration (CMC) (28). These micelles are fairly narrowly dispersed in size and contain up to 150 monomers. Micelles formed in anionic surfactant solutions are charged with the net charge being less than the aggregation number. The degree of dissociation is usually between 0.1 and 0.4.

The structure of these micelles has been the subject of much discussion (29). Figure 1 shows the surface tension isotherm at 25°C for sodium dodecyl sulfate (NaDS) measured by the Wilhelmy plate technique. Various investigators found different shapes of this isotherm in the region of the critical micelle concentration (CMC = 8×10^{-3} mole/liter). Based upon the shape of the surface tension isotherm in this transition region two primary mechanisms of micelle formation have been proposed: (1) When the transition region is smooth (see the isotherm marked by the circle), the mass action law of micelle formation is in effect, as Elworthy and Mysels show (30); (2) When the transition is sharper (see triangles), the micelle formation could be considered to produce a separate pseudophase, as the results of Sasaki *et al.* (31) show. According to our measurements, the shape of the isotherm in the transition region is closer to the model proposed by Sasaki *et al.* However, at aggregation numbers larger than 50, both these models give the same equilibrium constant for the micelle monomers.

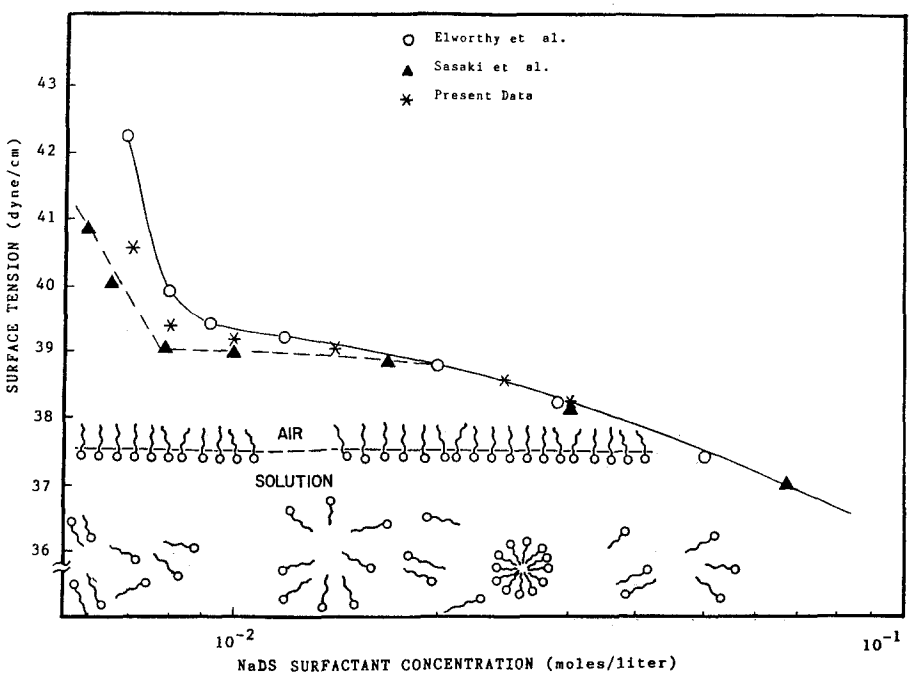

FIG. 1. Plot of the experimental data for the surface tension of a NaDS solution vs the surfactant concentration. The presence of surfactant monolayer at the surface and of the micelles in the bulk of the solution is illustrated schematically.

Reiss-Hussen and Luzzati (32) used the low angle X-ray technique and have established that in the concentration range of 0.03 to 0.10 mole/liter (which is the range of concentration used in our study) the micelles are spherical and that the micelle sphere-to-rod shape transition occurs at a concentration of 0.25 mole/liter at a temperature of 27°C. The polar radius of a micelle is 2.4 nm and the aggregation number is 67.

The micelles are in equilibrium with NaDS monomers, which are dissociated to Na^+ and DS^- ions into the solution. In this way, the NaDS monomers serve as electrolyte. The micelles are partially dissociated and the degree of dissociation in this concentration range is measured to be 27% (Sasaki *et al.*), i.e., 18 charges for a micelle. For this reason, the mean concentration of Na^+ ions in the solution is higher than the mean concentration of DS^- monomers (see Table I). C_{MIC}, the micellar concentration, reported in this table, has been calculated using the Hartley model (33), and assuming a spherical micelle structure with an aggregation number of 67. From the concentration of the micelles (as shown in Table I), one can calculate the volume per micelle. The cubic root of this volume yields the mean distance, δ_1, between the micelles in the bulk of the solution. The values of δ_1 for the different solutions are presented in Table I. The last column in this table tests the micellar volume fraction, ϕ.

(b) Measurements of the Film Thickness

In this section, we briefly describe the experimental procedure for calculating the stepwise thickness transitions in thin films formed from solutions of sodium *n*-alkyl sulfates.

To investigate the dynamic behavior of stratifying films, we used the reflected light interferometric technique described in Refs. (31–37). Microscopic films were formed in a cylindrical capillary with a hydrophilic inner wall of radius $R = 1.5$ mm. The films were formed by sucking out the liquid from a biconcave drop inside the capillary through an orifice in the wall. The resulting horizontal flat film is encircled by a biconcave meniscus. The radius of the film ($r_c = 0.3$ mm) is kept constant by controlling the capillary pressure, P_c, in the meniscus. In fact, the changes in P_c during the thinning of the film were negligible: in these experiments, $R \gg r_c$ and the contact angle subtended between the film and meniscus is less than 1°.

The glass cell assembly was enclosed in a thermostated environment and the temperature was maintained constant within ±0.2°C in the range of 20–50°C. The entire assembly was placed on the stage of a metallograph microscope (Model N11, Unitron Scientific Inc.) mounted on a vibration free table. The major problem in using the interference microscopic technique is eliminating the reflection from the meniscus around the film. This problem was overcome by choosing the proper objective aperture and field diaphragm and by using a fiber optic probe (Model 700-3B, Gamma Scientific Co.), positioned close to the film center (37). The light reflection from the bottom of the glass cell was eliminated by using an immersion objective. Monochromatic light (wavelength of 546 nm) was incident on the film surface, and the light reflected from a small portion of the film is conducted to a photomultiplier with the help of a fiber optic probe. The photocurrent is then recorded as a function of time. The experimental circuit is shown in Fig. 2.

The thickness of the film at any instant of time, t, was calculated from the intensity of photocurrent by an expression derived from (35, 36, 38):

$$h = \frac{\lambda}{2n_0\pi} \times \arcsin\left[\frac{\Delta}{1 + (4\beta/(1-\beta))(1-\Delta)}\right]^{1/2}, \quad [1]$$

where

$$\beta = \frac{n-1}{(n_0+1)}\left(\frac{n-n_0}{n+n_0}\right) \quad [2]$$

TABLE I

Data for Micellar Solutions of NaDS[a]

C_{NaDS} (mole/liter)	C_{Na^+} (mole/liter)	C_{DS^-} (mole/liter)	C_{MIC} (mole/liter)	δ_l (nm)	ϕ	σ^l (mN/m)
0.03	0.0123	0.0057	3.64×10^{-4}	16.6	0.0126	38.3
0.06	0.0192	0.0041	8.34×10^{-4}	12.6	0.029	37.3
0.08	0.0238	0.0030	1.15×10^{-3}	11.3	0.040	37.0
0.10	0.0284	0.0019	1.46×10^{-3}	10.4	0.051	36.6

[a] The concentrations C_{Na^+} and C_{DS^-} are taken from Ref. (31). δ_l is the mean distance between the micelles in the solution, ϕ is the micellar volume fraction, and σ^l is the surface tension of the bulk solution.

$$\Delta = \frac{I - I_{min}}{I_{max} - I_{min}}, \qquad [3]$$

where h is the film thickness which includes the thickness of the adsorbed layers, and n and n_0 are the refractive indices of the disperse phase and of the film. For a foam film, n is equal to 1.0, while n_0 was taken to be that for the aqueous solution. I is the instantaneous value of the photocurrent. I_{min} and I_{max} are its values at the last interferential minimum and maximum (see, for example, Fig. 3). λ is the wavelength of the monochromatic light used. Detailed information regarding the principles of light interferometry can be found in Ref. (39).

RESULTS AND DISCUSSION

Using films from micellar solutions, we observed the following phenomenon (see Fig. 3): After the film is formed, it immediately starts to decrease in thickness. When it becomes less than about 104 nm (after the last interferential maximum corresponding to the light reflected

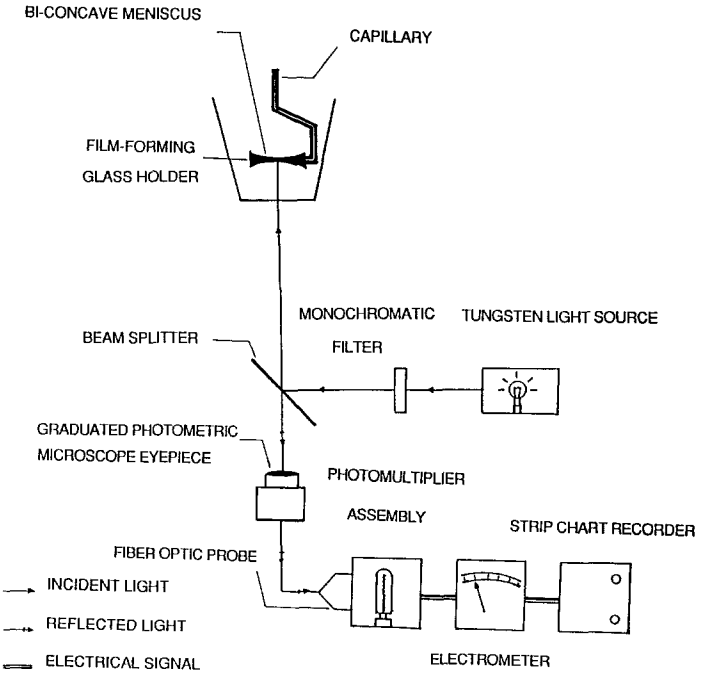

FIG. 2. Experimental setup for measurement of the film thickness.

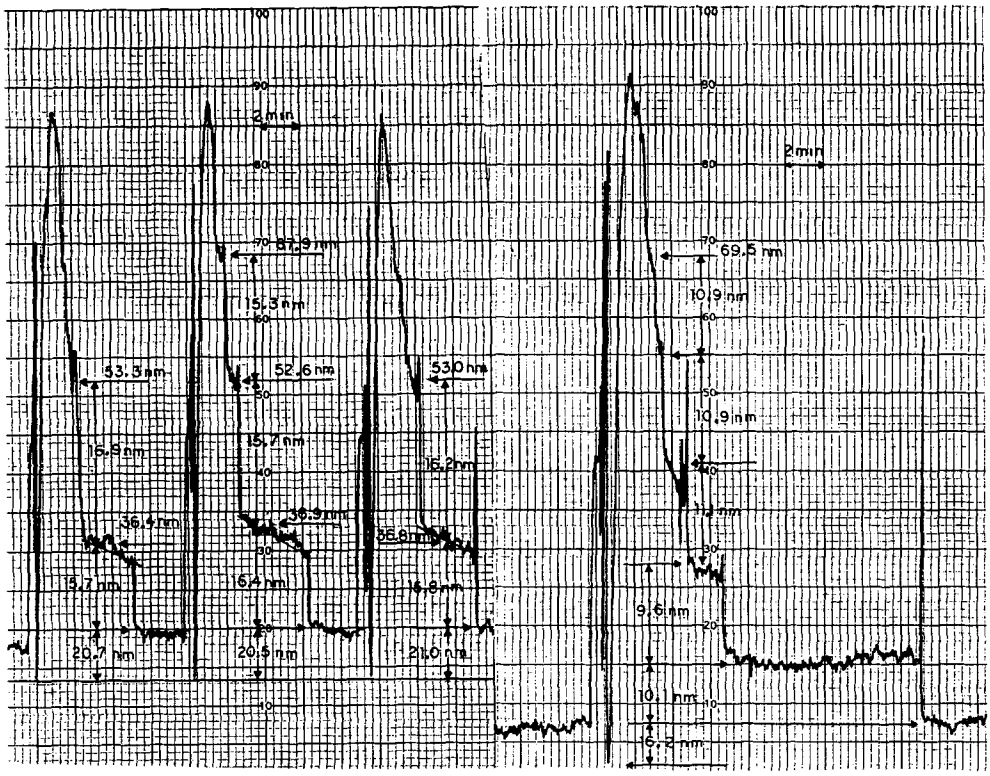

FIG. 3. Photocurrent vs time interferograms of thinning NaDS films at surfactant concentrations 0.03 mole/liter (the three curves on the left) and 0.1 mole/liter (the right curve).

from the film), the film thickness changes in several steps. The film first rests for a few seconds in a metastable state with uniform thickness. Then one or several dark spots (with less thickness than the remaining part of the film) appear and gradually increase in their area. Soon the spots cover the entire area of the film, and it rests for several seconds in a new metastable state. Then darker spots appear, and after their expansion a subsequent metastable state is reached. Finally, the film reaches a stable state and no more step-wise transitions occur. The metastable states of the film appear in the interferogram as steps whose width is proportional to the lifetime of the respective states. The estimated height of the steps is also shown in Fig. 3. The film thicknesses at the metastable states and their lifetimes, determined from Fig. 3, are presented in Table II, where $n = 0$ corresponds to the final stable state of the film. This table shows that the height of the step-wise thickness transition is approximately constant for all steps and its mean value, $\tilde{\delta}$, is dependent only on the surfactant concentration.

(a) Effect of Surfactant Concentration

Interferograms of thinning films formed from micellar solutions of NaDS for two sur-

TABLE II

Values of the Film Thickness, h_n, at the Metastable States and Their Lifetime, τ_n, Determined from the Interferogram in Fig. 3

n	h_n (nm)	τ_n (s)
0	16.2	—
1	26.3	600
2	35.9	108
3	47.0	36
4	57.9	24
5	68.8	19

factant concentrations (0.03 and 0.01 mole/liter) are presented in Fig. 3. The steps in the interferogram (after the last interferential maximum) reflect the step-wise thinning of the film. The height of the steps, $\tilde{\delta}$, is larger for the smaller NaDS concentration. This trend is illustrated in Table III with data for four different surfactant concentrations. The measured values of $\tilde{\delta}$ and of the final film thickness are plotted in Fig. 4 against the surfactant concentration.

The mean height of a step-wise film thickness transition, $\tilde{\delta}$, is between 15.8 and 10.4 nm (depending on the surfactant concentration). The micellar diameter has a value of 4.8 nm (32), which does not depend on the NaDS concentration (in this concentration range). In this case, $\tilde{\delta}$ should be compared with the Debye diameter of the electric double layer around a micelle rather than the diameter itself. Indeed, the width of the double layer around a micelle can be estimated to be of the order of the Debye–Huckel length $1/\kappa$ (11, 12), where

$$\kappa^2 = \frac{4\pi e^2 N_A}{10^3 \epsilon KT}(C_{Na} + C_{DS}).$$

Here N_A is Avogadro's number, K is the Boltzmann constant, ϵ is the solvent dielectric constant, e is the charge of an electron (in CGSE units), and C_{Na} and C_{DS} are the ionic concentrations (moles/liter). C_{Na} accounts for

TABLE III

Data for Solutions of Sodium Dodecyl Sulfate (NaDS)[a]

C_{NaDS} (mole/liter)	$\tilde{\delta}$ (nm)	δ_l (nm)	$2(R + (1/\kappa))$ (nm)	ψ_κ	ψ_0 (mV)
0.03	15.28	16.6	11.2	0.16	−79.2
0.06	11.8	12.6	10.4	0.30	−74.8
0.08	10.8	11.3	10.1	0.37	−72.3
0.10	10.4	10.4	9.7	0.42	−70.2

[a] $\tilde{\delta}$ and δ_l are the mean height of a step-wise film thickness transition and the mean distance beween the micelles in the solution. $2(R + 1/\kappa)$ is the diameter of a micelle together with its Debye atmosphere, and ψ_κ is the corresponding effective volume fraction of the micelles.

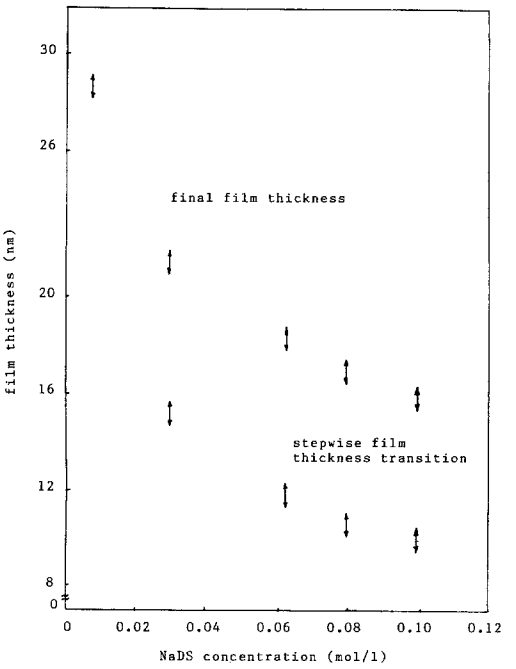

FIG. 4. The measured height of a step, $\tilde{\delta}$, and the final film thickness, h_0, as functions of the surfactant concentration.

the Na^+ ions dissociated both from the NaDS monomers and from the micelles (see Table I). The volume fraction of the micelles, including the Debye atmosphere around them, is shown in Table III. Table III also compares the height of a step, $\tilde{\delta}$, the diameter of the Debye atmosphere $2(R + (1/\kappa))$ around a micelle (R = 2.4 nm is the radius of the micelle itself), and the mean distance δ_l between the micelles in the bulk solution. All these quantities are very close to each other. Thus one can conclude that a step-wise decrease of the film thickness can be interpreted as removal of micelles one layer at a time from the film. In this way, the process of stratification can be considered as a layer-by-layer thinning of a micellar structure inside the film. It should be noted that in the investigated range of volume fractions of the micelles, structuring of charged particles in the bulk has been observed by many investigators (22–26).

From the viewpoint of the classical DLVO

theory (10, 11), the existence of such a structure can be explained by balance of the repulsive electrostatic forces and the attractive van der Waals forces between the micelles (see Ref. (17)). In other words, the pair interaction potential can be presented in the form

$$V = V^{el} + V^{vw}, \qquad [4]$$

where

$$V^{vw} = -\frac{A}{12}\left(\frac{1}{S + S^2/4} + \frac{1}{1 + S + S^2/4} + 2 \ln \frac{S + S^2/4}{1 + S + S^2/4}\right) \qquad [5]$$

$$V^{el} = \frac{\epsilon \psi_0^2}{2\kappa + H} \gamma \exp(-\kappa H) \qquad [6]$$

and

$$\psi_0 = \frac{e \cdot z}{\epsilon a(1 + \kappa R)}, \qquad [7]$$

Equation [5] is the expression of Hamaker for the van der Waals interactions between two equal sized spheres of radius R, separated by a distance H ($S = H/R$) from surface to surface. A is the Hamaker constant, z the number of charges per micelle, and ψ_0 the surface potential of a micelle. γ is a correction factor for the repulsion between two charged spheres (12). In our case, γ varies between 0.95 and 1.

Values of ψ_0, calculated from the Debye–Huckel expression [7], are shown in Table III. They allow the calculation of the interaction energy with the help of Eqs. [4]–[6]. The results, presented in Fig. 5, show that the separation distance H between the micelles is too large for the van der Waals forces to be important (note that in all cases we have $H = \delta_1 - 2R > 2R$; see Table III). Thus, the main conclusion is that the interaction between micelles, both in the bulk solution and in the thinning film, is due predominantly to the electrostatic repulsion. As known, this force can be strongly affected by adding electrolyte to the solution.

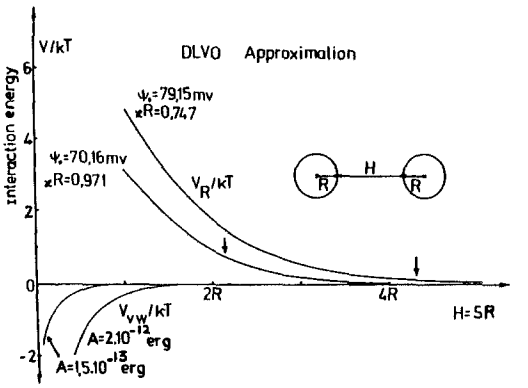

FIG. 5. Potential energies V^{el} and V^{vw} of the electrostatic repulsion between two micelles and of the van der Waals attraction between them. R is the radius of the micelles and H is the shorter distance between their surfaces.

(b) Effect of the Added Electrolyte

In our experiments, we added NaCl at different concentrations to the original NaDS solution. When the concentration of NaCl is increased, the number of the step-wise transitions decreases and becomes irregular (some of the steps are passed over). At sufficiently large electrolyte concentrations, there is only one transition, whose step height is dependent on the capillary pressure (i.e., the film radius). This concentration can be regarded as a threshold concentration, above which stratification phenomenon is not observed. This threshold is a function of both the electrolyte and the surfactant concentration. Our data for the effect of the electrolyte on the stratification are shown in Fig. 6. The curve, which represents the threshold concentration, separates the regions with and without stratification. The obvious conclusion is that the added electrolyte strongly suppresses the stratification (that is, there are no step-wise film thickness transitions).

The observed effect can be explained by the fact that the increased electrolyte concentration increases κ and decreases the width of the electric double layer around the micelles. The effective volume fraction of the micelles, accounting not only for the micelles but also for

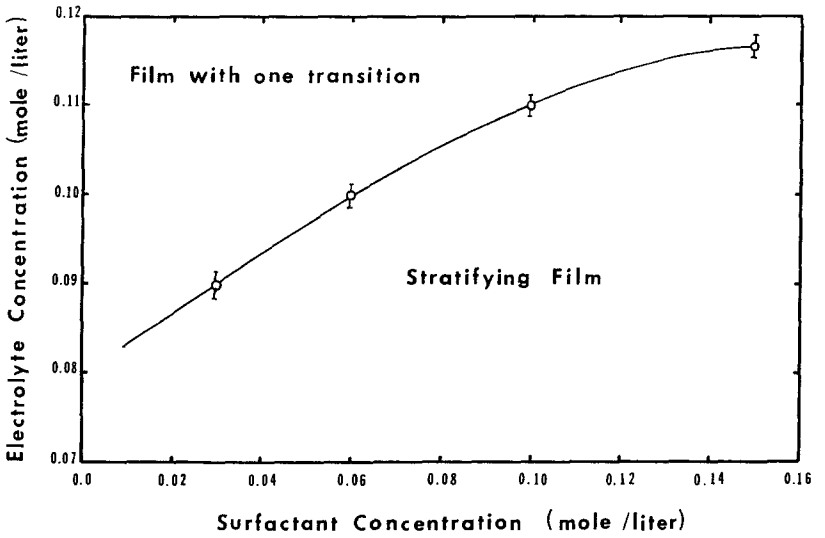

FIG. 6. Stratification–nonstratification phase diagram for NaDS with added NaCl.

the double layer volume, will strongly decrease, and formation of micellar structures inside the film will no longer be possible. In other words, the inhibition of the stratification by the added electrolyte can be interpreted as suppression of the micellar structure inside the film.

(c) Effect of the Surfactant Chain Length

To study the effect of the hydrocarbon chain length of the surfactant molecules on the stratification phenomenon, we investigated the thinning of films formed from aqueous solutions of sodium decyl, dodecyl, and tetradecyl sulfates (NaDeS, NaDS, NaTeDeS, respectively) at a concentration of 0.062 mole/liter with no added salt. The data are shown in Table IV. The most important effect is that increasing the chain length increases the number of observed transitions (this number is 4 for NaTeDeS, 3 for NaDS, and 2 for NaDeS). On the other hand, the height of a step is practically the same for all three surfactants.

The above phenomena can be explained by the increase in the number of micelles in the film. Indeed, it is known (29) that the longer hydrocarbon chain enhances micellization. Thus, at the same total concentration, the surfactant with a longer chain provides greater micellar concentration. The increased volume fraction of the micelles leads to the formation of micellar structures in the film with larger thicknesses. On the other hand, the change in

TABLE IV

Film Thicknesses of Stratifying Foam Films of Sodium *n*-Alkyl Sulfates

RSO_4Na[a] (0.062 mole/liter)	Film thicknesses of stratifying films (nm)				Final film thickness (nm)	Step-wise transition (nm)
NaDeS	36.2	24.2	—	—	17.9 ± 0.6	12.1 ± 0.6
NaLS	48.6	36.7	24.2	—	18.2 ± 0.5	12.2 ± 0.5
NaTeDeS	62.0	50.2	37.6	25.1	18.6 ± 0.4	12.4 ± 0.3

[a] NaDeS = Sodium decyl sulfate; NaDS = sodium dodecyl sulfate; NaTeDeS = sodium tetradecyl sulfate.

the chain length affects very slightly the effective volume fraction of the micelles because of the large volume of the Debye atmosphere around a micelle.

(d) Effect of the Capillary Pressure

The change in the pressure in the capillary meniscus affects the mechanical equilibrium between the film and the meniscus and leads to a change in the radius, r_c, of the contact line encircling the film. At small contact angles (less than 1° in the present study) and for perfect wetting of the capillary walls, r_c is related to the capillary pressure, P_c, by the equation (40)

$$P_c = \frac{2\sigma^1 R_c}{R_c^2 - r_c^2}, \qquad [8]$$

where σ^1 is the surface tension of the solution (the values of σ^1 are presented in Table I) and R_c is the inner radius of the capillary. Thus an increase in P_c leads to an increase in r_c and in the film area.

The change in the capillary pressure affects the occurrence of stratification. Our observations indicate that if P_c and r_c are increased, the step-wise thinning of the film is accelerated without any detectable change in the height of a step and in the number of the transitions. For example, the thinning of a film with radius $r_c = 0.3$ mm, from the last interference minimum to the final stable state, takes 336 s (see Fig. 7), whereas the same process takes 264 s for a film with $r_c = 0.4$ mm (in both cases, the concentration of NaDS being 0.03 mole/liter). This can be interpreted as an increase in the driving force of the film thinning with increased capillary pressure.

(e) Stratification with Latex Suspension

To verify that stratification is due to the presence of an ordered structure of (charged) particles inside the film, we also undertook a model experiment with a latex suspension. For this purpose, we used a 30 vol% aqueous solution of polystyrene latex (Dow Chemicals)

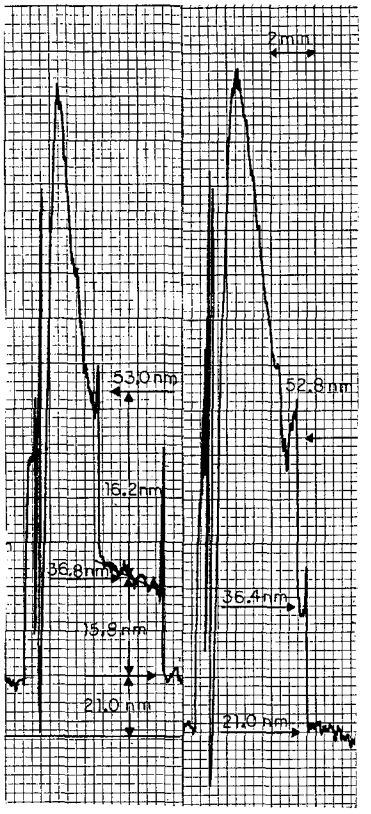

FIG. 7. Interferograms of thinning films for two different sizes.

with the diameter of a latex particle beling 91 ± 8 nm. As expected, we observed pronounced stratification with thinning films formed from this suspension. The process of step-wise thinning is illustrated with the series of photographs in Fig. 8. The bright area in Fig. 8a corresponds to a thickness $h = 281$ nm while the dark area has thickness $h = 190$ nm. The bright area decreases with time (Fig. 8b) and soon a uniform dark film has developed. Bright spots then begin to appear in the dark film (Fig. 8c); the measured thickness of these spots is 99 nm. They grow in size and cover the entire film area. Then dark spots with a thickness of 8 nm begin to appear in the uniformly bright film (Fig. 8d). This is the last transition, since the newly created uniform black film does not contain latex particles, and

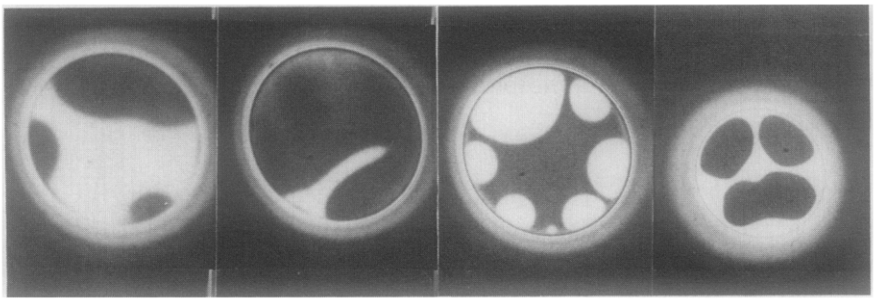

FIG. 8. Four successive photographs of the thinning of a liquid film formed from 30 vol% aqueous solution of polystyrene latex.

no change in the thickness of the film was detected. Thus, the average height of a step is 90 ± 2 nm, which coincides with the mean value of the particle diameter within experimental accuracy. One can then conclude that stratification is really a layer-by-layer thinning of an ordered structure of charged particles inside the film.

It is interesting to note that we observed both dark and bright spots in the thinning latex film, whereas only dark spots (with different intensities) were seen in films formed from micellar solutions. The appearance of bright spots is due to the large diameter of the latex particles. The thickness of a stratifying film containing such large particles exceeds the last interferential maximum, and thus both destructive and constructive interference occurred in this case.

CONCLUDING REMARKS

Using interferometric techniques, we studied the effect of different factors on the phenomenon of stratification. We established that an increase in the concentration of the anionic surfactant leads to an increase in the number of step-wise transitions, but to a decrease in the height of each step. In all cases where stratification is observed, we found that the height of each step is approximately equal to the mean distance between two ionic micelles in the solution. This distance is of the order of the diameter of a micelle together with the Debye atmosphere around it. The interaction between the micelles is due to the electrostatic repulsion between the Debye atmospheres; the van der Waals attractive forces are negligible at such large distances between the particles. Added salt suppresses the stratification and above a certain threshold salt concentration, no more step-wise transitions are observed. In addition, at the same concentration, a surfactant with longer hydrocarbon chain gives a more pronounced stratification (more step-wise transitions) without considerable effect on the height of a step. However, an increase of the capillary pressure does not affect the height of a step, but decreases the "lifetime" of a step and accelerates the process of stratification.

All these observations can be explained by suggesting that the stratification is due to the presence of micellar structuring inside the film and that the step-wise transitions are a layer-by-layer thinning of this structure. This hypothesis was supported by our model experiment with stratifying films containing latex particles. As we reported elsewhere (41), stratification can be caused not only by anionic

micelles and by latex particles in solutions, but also by micelles of nonionic surfactants. That is, the step-wise thinning is inherent in films containing particles which interact with repulsive forces.

The problem of how these repulsive forces can lead to structuring is not new. Special attention has been given to this problem after the experimental observations on ordering in latex (10, 23–27) and some biological suspensions (42, 43). The presence of order–disorder transitions in these systems above a certain volume fraction can be explained (17) by the fact that the particles are enclosed in a restricted space. The micelles in a thin film are also forced into a restricted volume environment, and in our opinion it is possible for micellar ordering to exist in the film even when such ordering is missing in the bulk solution.

To obtain a quantitative explanation of the experimental results reported here and to gain a deeper understanding of the stratification phenomenon, a theoretical study is needed based upon an appropriate molecular model. The idea for the presence of micellar ordering in a stratifying film provides a basis for such a model, which is developed in Part II of this study (44). We are presently investigating the mechanism of formation and expansion of dark spots and the related problem of the driving force for the stratification process.

ACKNOWLEDGMENTS

This study was supported in part by the National Science Foundation, the U.S. Department of Energy, and the Bulgarian Committee for Science and Technology.

REFERENCES

1. Johnnott, E. S., *Philos. Mag.* **70,** 1339 (1906).
2. Perrin, R. E., *Ann. Phys. (N.Y.)* **10,** 160 (1918).
3. Bruil, H. G., and Lyklema, J., *Nature* **232,** 19 (1971).
4. Kenskemp, J. W., and Lyklema, J., *ACS Symp. Ser.* **8,** 191 (1975) (Adsorption at Interfaces Pub. Symp. 1974).
5. Friberg, S., Linden, St. E., and Saito, H., *Nature* **251,** 494 (1974).
6. Manev, E., Proust, J. E., and Ter-Minassian-Saraga, L., *Colloid Polym. Sci.* **225,** 1133 (1977).
7. Manev, E., Sazdanova, S. V., and Wasan, D. T., *Dispersion Sci. Technol.* **5,** 111 (1984).
8. Kruglyakov, P. M., *Kolloidn. Zh.* **36,** 160 (1974).
9. Kruglyakov, P. M., and Rovin, I. G., "Physical Chemistry of Black Hydrocarbon Films—Bimolecular Lipid Membranes." Nauka, Moscow, 1978. [In Russian]
10. Hachisu, S., Kobayashi, Y., and Kose, A., *Colloid Interface Sci.* **42,** 342 (1973).
11. Derjaguin, B. V., and Landau, L. D., *Acta Physicochim. USSR* **14,** 633 (1941).
12. Verway, E. J. W., and Overbeck, J. Th. G., "Theory of Stability of Lyophobic Colloids." Elsevier, Amsterdam, 1949.
13. van Megen, W., and Snook, I., *J. Colloid Interface Sci.* **57,** 40 (1976).
14. Snook, I., and van Megan, W., *J. Colloid Interface Sci.* **57,** 47 (1976).
15. Snook, I., and van Megen, W., *J. Chem. Soc., Faraday Trans. 2* **72,** 216 (1976).
16. Marcelja, S., Mitchell, D. J., and Ninham, B. W., *Chem. Phys. Lett.* **43,** 353 (1976).
17. Efremov, I. E., *in* "Surface and Colloid Science" (E. Matijevic, Ed.), Vol. 8, p. 40. Wiley, New York, 1978.
18. Ohtsuki, T., Mitaku, S., and Okano, K., *Japan. J. Appl. Phys.* **17,** 627 (1978).
19. Ruff, I., Palinkas, G., and Gombos, K., *J. Chem. Soc., Faraday Trans. 2* **77,** 1189 (1981).
20. Ottewill, R. H., *in* "Colloidal Dispersions" (J. W. Goodwin, Ed.). Special Publication, Royal Soc. London, London, 1982.
21. Duckinson, E., *in* "Specialist Periodical Reports Colloid Science" (D. H. Everett, Ed.), Vol. 4. Royal Soc. Chem., London, 1983.
22. Castillo, C. A., Rajagopalan, R., and Hirtzel, C. S., *Rev. Chem. Eng.* **2,** 239 (1984).
23. Clint, G. E., Clint, J. H., Corkill, J. M., and Walker, T., *J. Colloid Interface Sci.* **44,** 121 (1973).
24. Kose, A., Ozaki, M., Takano, K., Kobayashi, Y., and Hachisu, S., *J. Colloid Interface Sci.* **44,** 330 (1973).
25. Brown, J. C., Pusey, P. N., Goodwin, J. W., and Ottewill, R. H., *J. Phys. A: Math. Gen.* **8,** 664 (1975).
26. Brown, J. C., Goodwin, J. W., Ottewill, R. H., and Pusey, P. N., *in* "Colloid Interface Science" (M. Kerker, Ed.), Vol. 4, p. 59. Academic Press, New York, 1976.
27. Furusawa, K., and Tomotsu, N., *J. Colloid Interface Sci.* **92,** 504 (1983).
28. McBain, J. W., *Trans. Faraday Soc.* **9,** 29 (1913).
29. Shinoda, K., Nakagawa, T., Tamamushi, B., and Isemuva, T., *in* "Colloidal Surfactants: Some Physicochemical Properties." Academic Press, New York, 1963.

30. Elworthy, P. H., and Mysels, K. J., *J. Colloid Interface Sci.* **21,** 331 (1966).
31. Sasaki, T., Halton, M., Sasaki, J., and Nuking, K., *Bull. Chem. Soc. Japan* **148,** 1397 (1975).
32. Reiss-Husson, F., and Luzzati, V., *J. Phys. Chem.* **63,** 1969 (1959).
33. Hartley, G. S., "Aqueous Solutions of Paraffin-Chain Salts." Hermann, Paris, 1936.
34. Derjaguin, B. V., and Titievskaya, A., *Discuss. Faraday Soc.* **18,** 27 (1954).
35. Scheludko, A., *Kolloidn. Zh.* **155,** 39 (1957).
36. Lyklema, I., Scholten, P. S., and Mysels, K., *J. Phys. Chem.* **69,** 116 (1965).
37. Rao, A. A., Wasan, D. T., and Manev, E. D., *Chem. Eng. Commun.* **15,** 63 (1982).
38. Frankel, S. P., and Mysels, K. J., *J. Appl. Phys.* **37,** 3725 (1966).
39. Vasicek, A., *in* "Optics of Thin Films." North-Holland, Amsterdam, 1960.
40. Toshev, B. V., and Ivanov, I. B., *Ann. Univ. Sofia (Fac. Chem.)* **65,** 329 (1970/1971).
41. Wasan, D. T., and Nikolov, A. D., Lecture presented at the VIth International Symposium on Surfactants in Solution, New Delhi, 1986.
42. Parsegian, V. A., and Brenner, S. L., *Nature* **259,** 632 (1976).
43. Ise, N., and Okubo, T., *Acct. Chem. Res.* **13,** 303 (1980).
44. Nikolov, A. D., Kralchevsky, P. A., Ivanov, I. B., and Wasan, D. T., *J. Colloid Interface Sci.* **132** (1989).